

EFFECT OF ENCAPSULATING MATERIALS ON DETECTION OF AMMONIUM NITRATE EXPLOSIVES

NGUSHA T. A^{1*}, AMAH A. N², ONOJA A. D.³

Physics Department, University of Agriculture, Makurdi, Nigeria

*ngushaalmighty@gmail.com, +2347088294975

Keywords: Explosive, Ammonium nitrate, Container, Thickness, Detection, MCNP

Abstract. The study investigated the effect of encapsulating materials (containers) on detection of ammonium nitrate explosives. Fast neutrons analysis was employed in interrogating the explosive encapsulated in ceramic, HDPE, steel and wooden containers having thicknesses ranging from 0.5 cm to 5 cm. The study was carried out by means of computer simulation using MCNP simulation code. Key findings of the work include an inverse proportionality relationship between detection and container thickness. Steel containers were found to attenuate detection the most while wooden containers were the least affected by a unit increase in thickness. All materials studied were seen to attenuate detection by more than 70% at 0.5 cm thickness.

1.0 Introduction

Over the last few decades, the world has witnessed an overwhelming rise in terrorism. As at the year 2015, the Global Terrorism Index (GTI) identifies over 162 nations of the world grappling with issues relating to terrorism [1]. The nation Nigeria has not been spared as it currently battles an unprecedented surge of terrorist acts with the dreaded group commonly referred to as Boko Haram (BH) claiming responsibility for the bulk of attacks.

The GTI report indicates that explosives, bombs and dynamite constitute 60 per cent of global terrorist weapons. Firearms constitute 30 per cent while the use of other tactics including incendiary devices, melee attacks and sabotage of equipment make up 10 per cent [1]. The use of explosives is clearly favoured by terrorist groups as it greatly enhances the lethality of attacks. BH attacks were perpetrated mainly by means of fire arms using machine guns until 2014 when the use of explosives became dominant [1]. Their recourse to bombings according to the GTI greatly increased the lethality of the group so much so that they were ranked as the most dreaded terrorist group for the year 2014.

Binnie and Wright [2] in small arms survey ranks ammonium nitrate (AN) as the world's most common explosive used by terrorists. The preference for AN explosive may not be unconnected to the ready availability of its precursor in the form of ammonium nitrate fertilizer as well as the ease with which the explosive may be synthesized from the precursor and fuel oil. As is to be expected, efforts are on globally to develop techniques for the detection of these devices. This is partly responsible for the current wave of improvisations been made to explosive devices. Improvisations relating to the container in which these explosives are encapsulated are very prevalent as the need to conceal the devices from both human observers and explosive detectors is compelling.

Current best practices in explosive detection involve the use of neutron based technologies. The effectiveness of these technologies according to the National Research Council [3] is however beset by "background problems" arising from the activation of other materials in the vicinity of the explosive. Of these activated extraneous materials, the container in which the explosive is packed constitutes its most pervasive background and will as such greatly affect the detection of contained explosive. It thus becomes necessary to investigate the effect of container materials on the detection of contained ammonium nitrate explosive.

This study will address this problem by interrogating AN explosive enclosed in containers by fast neutron analysis. Selection of container materials to be investigated will be done so as to cover all classes of engineering materials. The sodium iodide detector will be employed for capture of the emitted gamma photons.

2.0 Theory

2.1 Neutron Transport through Materials. The problem of encapsulated explosive detection by means of fast neutrons is that of coupled neutron/photon transport through matter. The physics of particle and radiation transport through materials has been established for many years and is aptly captured by Lamarsh and Baratta [4], James [5], as well as several other authors.

Consider the transport of a neutron N (representing any number of particles) released from a neutron source. The particle starts off with an initial energy E and is located at the initial position r . It moves in a straight line from the source with its direction of travel represented by the vector (Ω) . If a target is placed on the path of its journey, the neutron undergoes an interaction (i) with a nucleus in the target. Interactions occurring upon collision of neutrons and nuclei in the target may either be elastic or inelastic scatterings, capture or fission interaction.

The normalized scattering kernel captures the probability of scattering interactions(both elastic and inelastic) by

$$\int_0^{\infty} dE \int_{4\pi} d\Omega \Sigma_s(\Omega' \cdot \Omega, E' \rightarrow E) = 1 \quad (1)$$

Equation (1) which represents the fractional probability of scattering from direction Ω' and energy E' to direction range $d\Omega$ and energy range dE indicates that scattering is a function of the scattering cross section (Σ_s) and depends only on the energy of the incident neutrons and the cosine of the angle between the incoming direction (Ω') and scattered neutron directions (Ω).

When collision results in fission interactions, daughter neutrons are produced isotropically and appear in the direction and energy range ($\Delta\Omega$ and ΔE) according to the distribution $\chi(E)$, where the fractional probability of a fission neutron (P_{fn}) appearing in the stated direction and energy range is given by:

$$P_{fn} = \frac{\chi(E)}{4\pi} \Delta\Omega \Delta E \quad (2)$$

The daughter neutrons produced undergo collision again and may repeat the same cycle or along with the initial neutrons may undergo capture leading to their annihilation.

As interaction occurs, neutrons are gained and lost in the interaction volume space (V). The number of particles lost from the system (P_L) due to scattering out of the direction, energy and volume range $V\Delta\Omega\Delta E$ is given by

$$P_L = \Delta\Omega\Delta E\Delta t \int_V dr \Sigma_s(r, E, t) \phi(r, \Omega, E, t) \quad (3)$$

The total gain from fissions(P_G) in $V\Delta\Omega\Delta E$ is given by

$$P_G = \Delta\Omega\Delta E\Delta t \int_V dr \frac{\chi(E)}{4\pi} \int_0^{\infty} dE' \int_{4\pi} d\Omega' v(E') \Sigma_f(r, E', t) \phi(r, \Omega', E', t) \quad (4)$$

Summing all interaction processes including contributions and losses and taking the limit as Δt , $\Delta\Omega$ and ΔE approach 0 gives the overall particle balance at any time t as

$$\begin{aligned} & \int_V dr \left\{ \left[\frac{1}{v} \frac{\partial}{\partial t} + \Omega \cdot \nabla + \Sigma(r, E, t) \right] \phi(r, \Omega, E, t) - \right. \\ & \int_0^{\infty} dE' \int_{4\pi} d\Omega' \Sigma_s(r, \Omega' \cdot \Omega, E' \rightarrow E) \phi(r, \Omega', E', t) - \\ & \left. \frac{\chi(E)}{4\pi} \int_0^{\infty} dE' \int_{4\pi} d\Omega' v(E') \Sigma_f(r, E', t) \phi(r, \Omega', E', t) \right\} = 0 \end{aligned} \quad (5)$$

Assuming a continuous integrand, the above integral is zero only if the integrand is zero. This assumption yields the Boltzmann transport equation

$$\left[\frac{1}{v} \frac{\partial}{\partial t} + \Omega \cdot \nabla + \Sigma(r, E, t) \right] \phi(r, \Omega, E, t) = \int_0^\infty dE' \int_{4\pi} d\Omega' \Sigma_s(r, \Omega' \cdot \Omega, E' \rightarrow E) \phi(r, \Omega', E', t) + \frac{\chi(E)}{4\pi} \int_0^\infty dE' \int_{4\pi} d\Omega' v(E') \Sigma_f(r, E', t) \phi(r, \Omega', E', t) \quad (6)$$

As $t \rightarrow \infty$, we may integrate equation 6 over all time to yield

$$[\Omega \cdot \nabla + \Sigma(r, E)] \phi(r, \Omega, E) = \int_0^\infty dE' \int_{4\pi} d\Omega' \Sigma_s(r, \Omega' \cdot \Omega, E' \rightarrow E) \phi(r, \Omega', E') + \frac{\chi(E)}{4\pi} \int_0^\infty dE' \int_{4\pi} d\Omega' v(E') \Sigma_f(r, E') \phi(r, \Omega', E') \quad (7)$$

Equation (7) is a form of Boltzmann's transport equation independent of time. It aptly captures the transport of neutrons through matter but assumes a thin target. For real targets, equation (7) must be modified to accommodate the exponential decay of source particle intensity as it travels through a thick target.

If we consider the neutron beam with N neutrons per cm^3 travelling from the source with speed 'v', the intensity of the beam as it leaves the source is given by

$$I = Nv \quad (8)$$

As the beam travels, it encounters the target with thickness X . Assuming X is composed of a theoretically finite number of thin layers each having thickness dx , then the beam interacts with the first layer with an interaction density (F) given by

$$F = IN\sigma_t \quad (9)$$

Where σ_t is the total microscopic cross section and is the sum of all cross sections. $N\sigma_t$ is the total macroscopic cross section and is usually represented by Σ_t .

This interaction with the first dx layer of the target attenuates the intensity of the beam $I(x)$ incident on the layer dx by

$$-dI(x) = \Sigma_t I(x) dx \quad (10)$$

The intensity of the uncollided beam available for interaction with the next dx thin layer is given by

$$I(x) = I_0 e^{-\Sigma_t x} \quad (11)$$

Where I_0 is the initial intensity of the beam. It should be observed that as the thickness of the target increases, the distance x increases proportionately conveying the idea of more dx layers and therefore an exponential decrease in neutrons available for interaction as thickness increases. This decrease in

interacting neutrons with thickness will no doubt affect the effectiveness of neutron interrogation as thickness increases.

If we introduce equation (11) with the term 'I' into the transport equation of equation (7), the modified transport equation capturing the transport of neutrons becomes

$$\begin{aligned}
 & [\Omega \cdot \nabla + \Sigma(r, E)]\phi(r, \Omega, E) = \\
 & \int_0^\infty dE' \int_{4\pi} d\Omega' \Sigma_s(r, \Omega' \cdot \Omega, E' \rightarrow E)\phi(r, \Omega', E') + \\
 & \frac{\chi(E)}{4\pi} \int_0^\infty dE' \int_{4\pi} d\Omega' v(E')\Sigma_f(r, E')\phi(r, \Omega', E') + I(r, \Omega, E)
 \end{aligned} \tag{12}$$

2.2 Neutron Induced Photon Production. When a neutron interacts with a nucleus in the target material, inelastic gamma photons having energies unique to the interacting nucleus is produced. The emitted photon travel through the material and experience attenuation according to equation (11).

Integrating equation (11) over all dx layers gives the gamma photon intensity at the posterior end of the thick target material as

$$I(X) = I_0 e^{-\Sigma_t X} \tag{13}$$

The intensity represented by equation (13) may be captured by a gamma ray detector and is useful in analysing the elemental composition of interrogated targets. This is especially important when dealing with explosives enclosed in containers. The high penetrating neutrons interrogate the explosive target releasing characteristic photons which are captured by a detector. Analyses of captured photons would usually reveal if detection was achieved or not. Literature [6, 7] gives the explosive signifying elements and their characteristic energies induced by fast neutrons as Carbon (4.4390 MeV), Nitrogen (5.1059) and Oxygen (6.1299).

3.0 Experimental Work

The investigation undertaken by this study was carried out by means of computer simulation using version 4c of the Monte Carlo N-Particle simulation code (MCNP). MCNP is a particle transport code developed at the Los Alamos National Laboratory. It is a general-purpose Monte Carlo transport code that can be used to simulate the process of neutron interaction with matter [8].

In simulating particle transport using the code, the user creates an input file that is read by MCNP. This file contains information about the problem in areas such as the geometry specification, the description of materials, the selection of cross-section evaluations, the location and characteristics of the source as well as the type of answers or tallies desired.

Specifically, the user creates three-dimensional geometries by defining cells bounded by surfaces. The user then specifies the materials that occupy cells in terms of their density and the atomic fraction of the elements comprising them. Elements are specified by means of unique identifiers known as ZAID. The MCNP code incorporates a regularly updated library of nuclear and atomic data in the Evaluated Nuclear Data File (ENDF) system. As such, specifying elements by their ZAID calls up all associated nuclear parameters for the material. The source and tallies are then specified. A tally scores events similar to an actual detector with perfect efficiency.

3.1 Simulated Materials. The materials simulated in this study are listed followed by a brief description

- i. Neutron source: The neutron source is point isotropic producing 14.1 MeV mono-energetic neutrons at strength of 10^{11} n/s.
- ii. Gamma-ray detector: Sodium iodide (NaI) scintillation detectors were utilized.
- iii. Explosive: Ammonium nitrate explosive composition (AN) with the chemical formula NH_4NO_3 and density of 1.72g/cm^3 .
- iv. Encapsulating materials (containers):
Four (4) materials were used in the study. Materials were selected to represent the four classes of engineering materials with a material drawn from each class. These were:
 - a) ceramic (fired clay) with density of 2.403g/cm^3
 - b) carbon steel with density of 7.82g/cm^3
 - c) oak wood with density of 0.67g/cm^3
 - d) high density polyethylene (HDPE) with density of 0.93g/cm^3 .

3.2 Method. The experiment is set up as shown in Figure 1. A cylindrical container houses the explosive charge and is located between a neutron source and a sodium iodide detector. With respect to the Cartesian coordinate reference system, the container is centred on the origin with its centre coordinates at (0 0 0). The horizontal length (L) of the cylinder is centred on the arbitrarily defined y axis and extends equal distances to the left and right from its centre point while its height (equivalent to its

diameter) rises in the z direction. The container with a length (L) of 94 cm and an internal radius (r) of 20 cm has a volume accommodating 200 kg of AN explosive. The thickness of the container (t) is varied by adjusting its external radius (R) where R is a sum of the internal radius and the desired thickness.

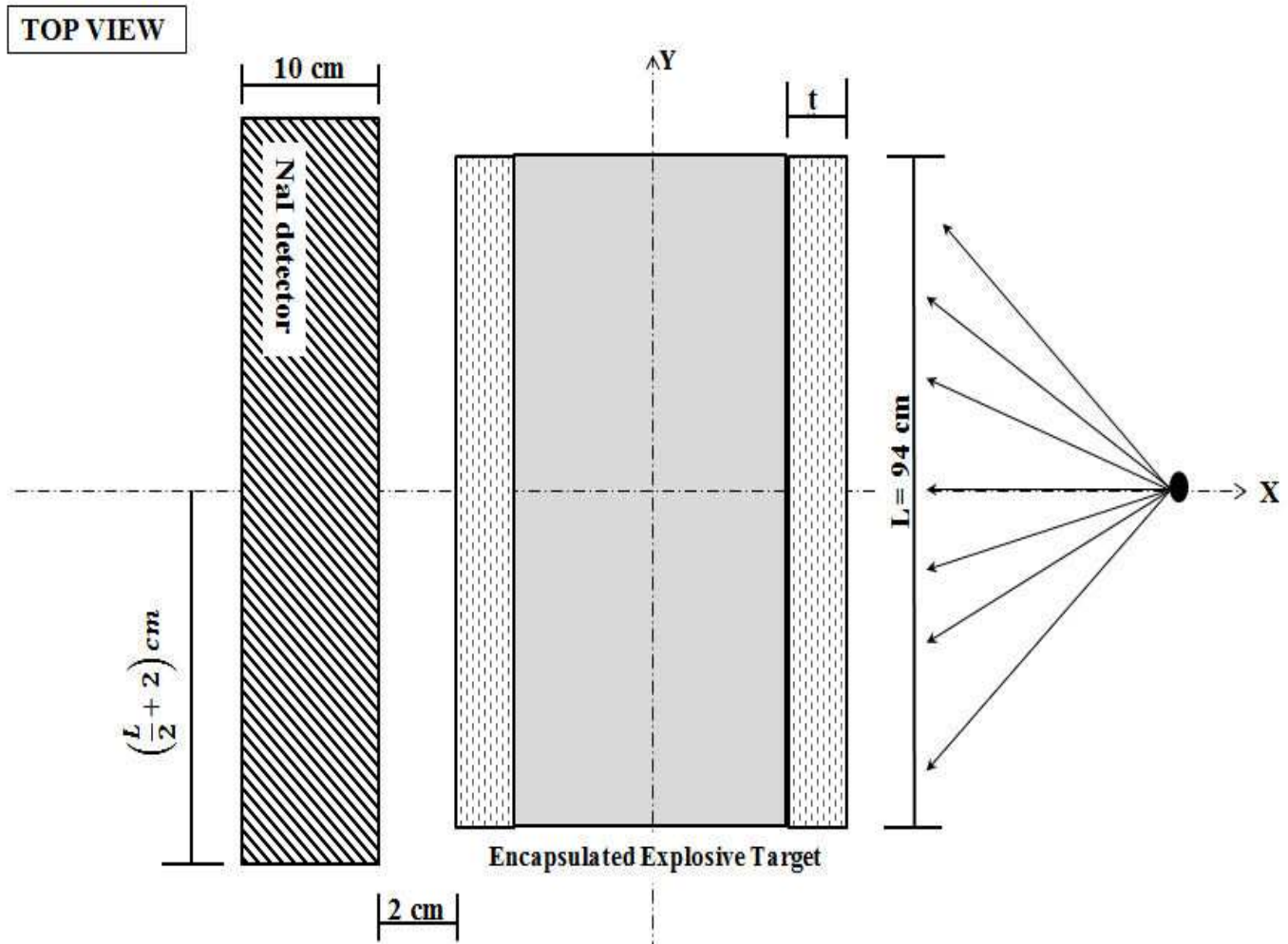


Figure 1a: Top view of the experimental setup

The experiment is set up as shown in Figures 1a and b. A cylindrical container houses the explosive charge and is located between a neutron source and a sodium iodide detector. With respect to the Cartesian coordinate reference system, the container is centred on the origin with its centre coordinates at (0 0 0). The horizontal length (L) of the cylinder is centred on the arbitrarily defined y axis and extends equal distances to the left and right from its centre point while its height (equivalent to its diameter) rises in the z direction. The container with a length (L) of 94 cm and an internal radius (r) of 20 cm has a volume accommodating 200 kg of AN explosive. The thickness of the container (t) is varied by adjusting its external radius (R) where R is a sum of the internal radius and the desired thickness.

The source is point isotropic and emits 14.1 MeV neutrons at a rate of 10^{11} ns^{-1} . Placed to the right of the cylinder; it is located at a constant distance (d) of 50 cm measured from the centre of the explosive charge and having coordinates (50, 0, 0). The detector is a rectangular sodium iodide bar located 2 cm behind the cylindrical explosive container. The detector has a thickness of 10 cm with its length extending 2 cm beyond the left and right ends of the cylinder and 1 cm above and below the height of the cylinder.

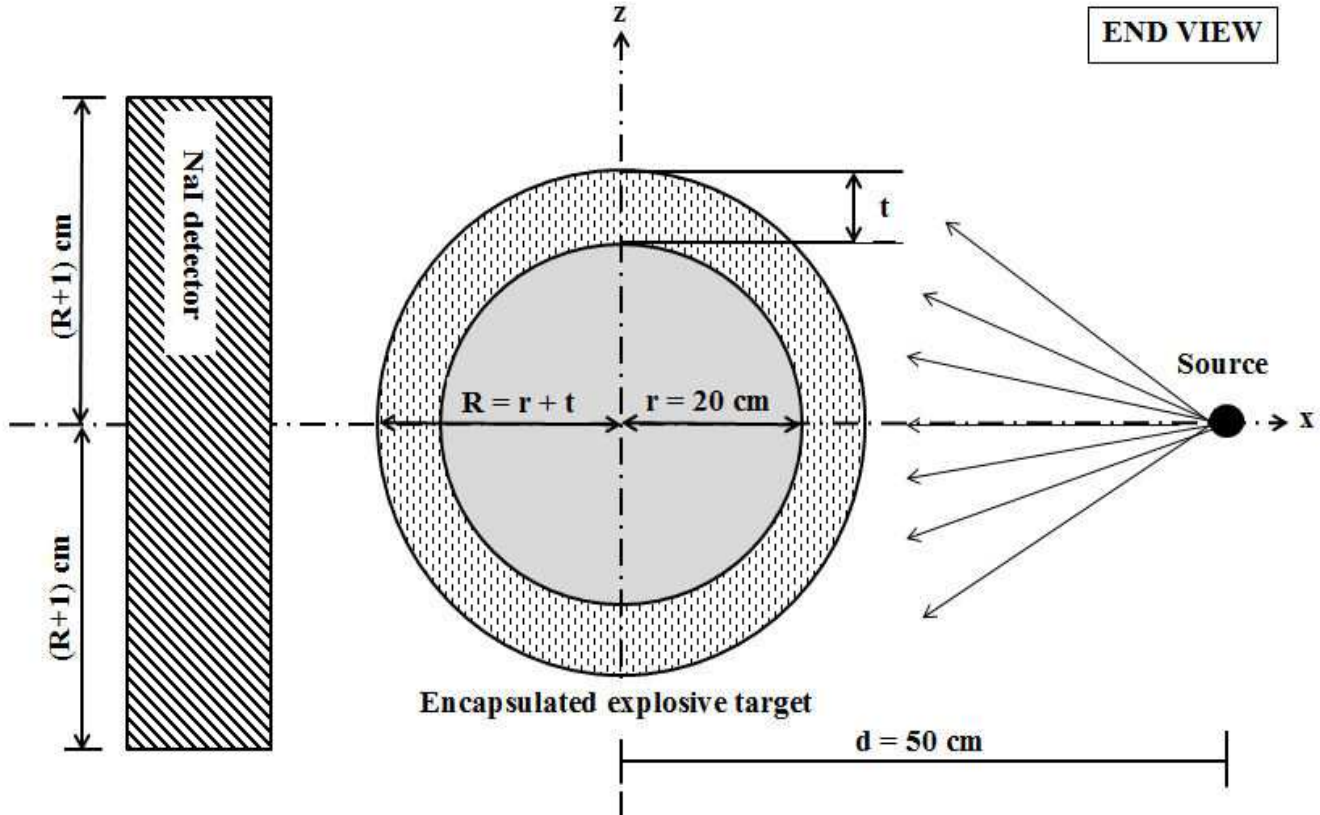


Figure 1b: End view of the experimental setup

Four sets of neutron interrogation were carried out; one each for cylinder containers made of ceramic, high density polyethylene (HDPE), carbon steel and oak wood. Container thickness considered in each set ranged from 0.5 cm through 5 cm in increments of 0.5 cm. Two hundred million neutron particle histories were run in every instance and the F4 tally of MCNP was used to tally photon output. The tallies obtained by the NaI detector were modified to incorporate a Gaussian experimental detector response function using FT GEB -0.015 0.118 0.

4.0 Result and Discussion

AN as a hydrogen based explosive is identified by its elemental stoichiometry of carbon (C), nitrogen (N) and oxygen (O) when interrogated by fast neutrons. In this research work, the magnitude of each of these elements is captured by the sodium iodide detector and the sum of C, N and O computed to yield the

quantity known as material quotient (MQ). MQ values indicate the intensity to which a material is identical to an explosive substance

Table 1 presents the result for the interrogation of 200 kg of AN explosive. The detector photon count for carbon (2.56E-07), nitrogen (3.60E-08) and oxygen (6.14E-08) is tabulated along with the value of the material quotient MQ (3.53E-07). Tables 2-5 present values for the interrogation of the same 200 kg of explosive when it is packed in containers of varying thicknesses. The tables feature a compilation of MQ values, percentage deviation of computed MQ from that of the unpacked explosive and the range (difference between highest MQ and lowest MQ value) for each container material studied.

Table 1: Result for the interrogation of 200kg of Ammonium nitrate

Parameter	Signature energy (MeV)	Magnitude (Photon count)
C	4.4390	2.56E-07
N	5.1059	3.60E-08
O	6.1299	6.14E-08
MQ		3.53E-07

An examination of tabulated values shows an MQ value of 3.53E-07 for unpacked AN. This is far different from any of the MQ values presented in tables 2-5 thereby establishing superficially that encapsulating an explosive affects its detection. A survey of trends for the encapsulated explosives indicates that MQ decreases as container thickness increase. This immediately establishes an inverse proportionality relationship between container thickness and detectability. The relationship is indicative of an increasing difficulty in detection with increasing container thickness. Figures 2- 5 which are graphs of MQ plotted against material thickness for the four packaging materials investigated clearly captures this relationship.

At 0.5 cm container thickness where measurement began, MQ value of 9.47E-08 was obtained for ceramic, 9.38E-08 for HDPE, 8.69E-08 for steel and 9.53E-08 for wood. These values are far below the value of the unpacked explosive thus indicating attenuation in detectability with encapsulation. Comparing these values with the 3.53E-07 MQ of the unpacked explosive, the 0.5 cm thick explosive container is seen to have attenuated detection by 75.42% for steel containers, 73.46% for HDPE, 73.21% for ceramic and 73.03% for wood. The values reveal an approximate 2% higher attenuation for steel encapsulation. This is to be expected as steel features relative high Z values and a high material density.

These along with variation in macroscopic cross sections are responsible for the varying attenuation intensities observed for the four encapsulation materials.

Table 2: Values for the interrogation of 200 kg of AN Explosive contained in ceramic containers of varying thickness

THICKNESS (cm)	0.5	1	1.5	2	2.5	3	3.5	4	4.5	5	MEAN
MQ (E-08)	9.47	9.32	8.99	8.68	8.38	8.08	7.76	7.45	7.19	6.89	8.22
%DMQ	73.19	73.62	74.57	75.44	76.29	77.14	78.03	78.92	79.65	80.5	76.74
Range	2.58										

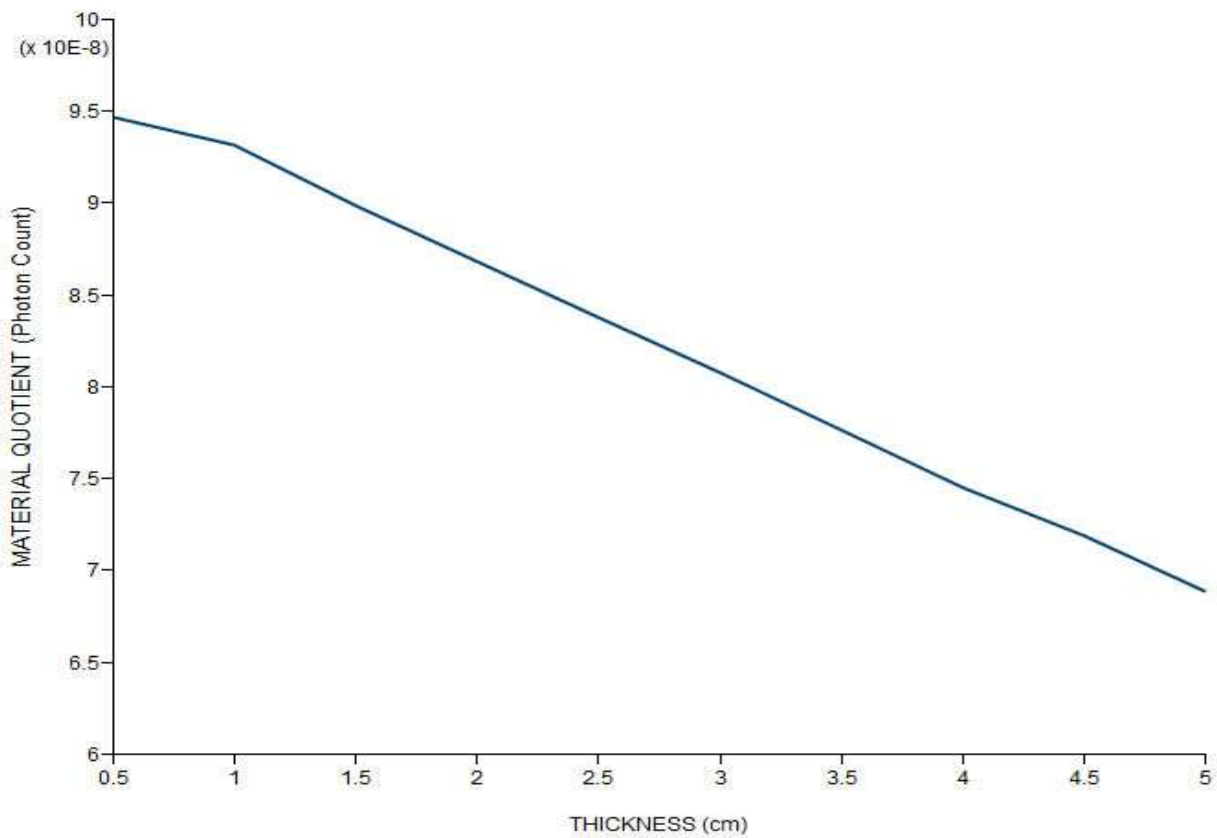


Figure 2: MQ variation with thickness for Ceramic containers

Computations of average MQ values return 8.22 mean MQ for ceramic, 8.09 for HDPE, 5.12 for steel and 9.07 for wood. On a general note therefore, detection of explosives contained in encapsulating materials having thicknesses between 0.5 cm and 5 cm is lowest for steel encapsulation followed by HDPE, ceramic and wood in that order. The disparity in mean values is not negligible as a 43.55% difference exists between the values of steel and wood indicating primarily that attenuation in steel containers is about double that of wood. This implies that the detection of AN explosive in wooden containers is approximately twice more likely than those contained in steel.

Table 3: Values for the interrogation of 200 kg of AN Explosive contained in HDPE containers of varying thickness

THICKNESS (cm)	0.5	1	1.5	2	2.5	3	3.5	4	4.5	5	MEAN
MQ (E-08)	9.38	9.17	8.88	8.56	8.22	7.9	7.62	7.33	7.05	6.77	8.09
%DMQ	73.44	74.06	74.88	75.78	76.74	77.65	78.44	79.27	80.06	80.86	77.12
Range	2.61										

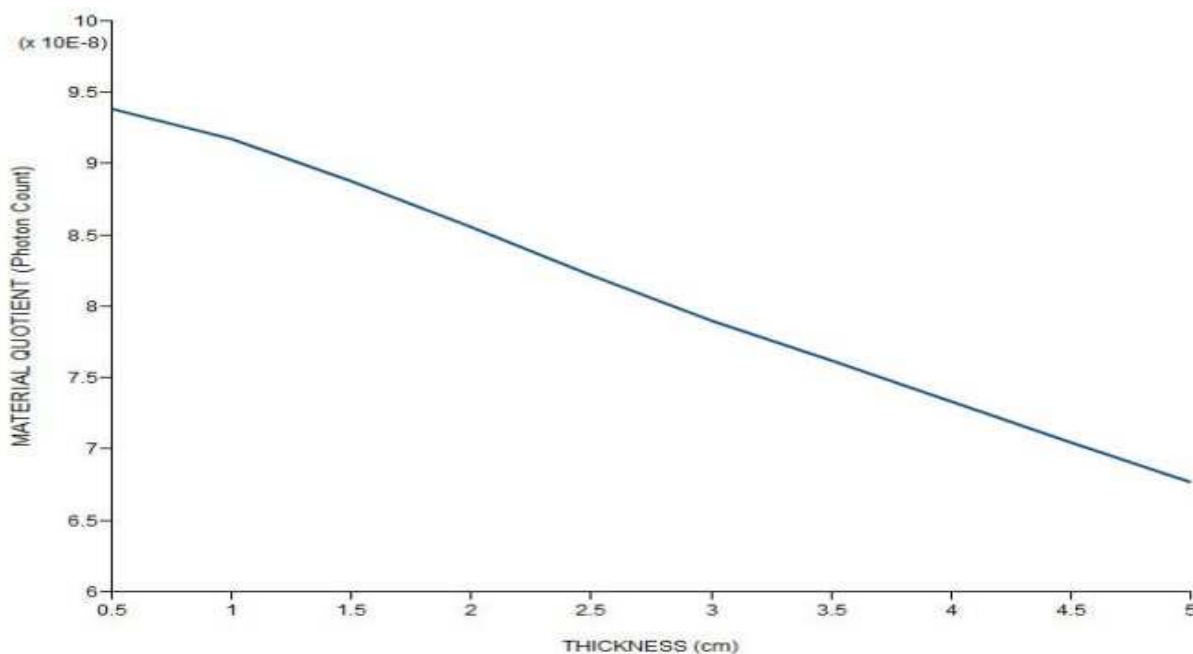


Figure 3: MQ variation with thickness for HDPE containers

The tabulated range was computed by taking the difference between the highest and lowest observed MQ values for each category of interrogation. The range being a measure of dispersion attempts to estimate the level to which the encapsulated explosive reacts to variation in container thickness. Between 0.5 cm and 5.0 cm, ceramic featured values spanning through a range of 2.58. HDPE featured a range of 2.61 while steel and wood featured a range of 6.24 and 0.90 respectively. From the stated values, it is observed that wood presented a strikingly narrow range while steel returned a noticeably broad range. HDPE and ceramic on the other hand had ranges with negligible difference.

Table 4: Values for the interrogation of 200 kg of AN Explosive contained in steel containers of varying thickness

THICKNESS (cm)	0.5	1	1.5	2	2.5	3	3.5	4	4.5	5	MEAN
MQ (E-08)	8.69	7.8	6.8	5.91	5.1	4.42	3.85	3.34	2.87	2.45	5.12
%Div	75.42	77.91	80.74	83.28	85.56	87.48	89.11	90.55	91.89	93.07	85.50
Range	6.24										

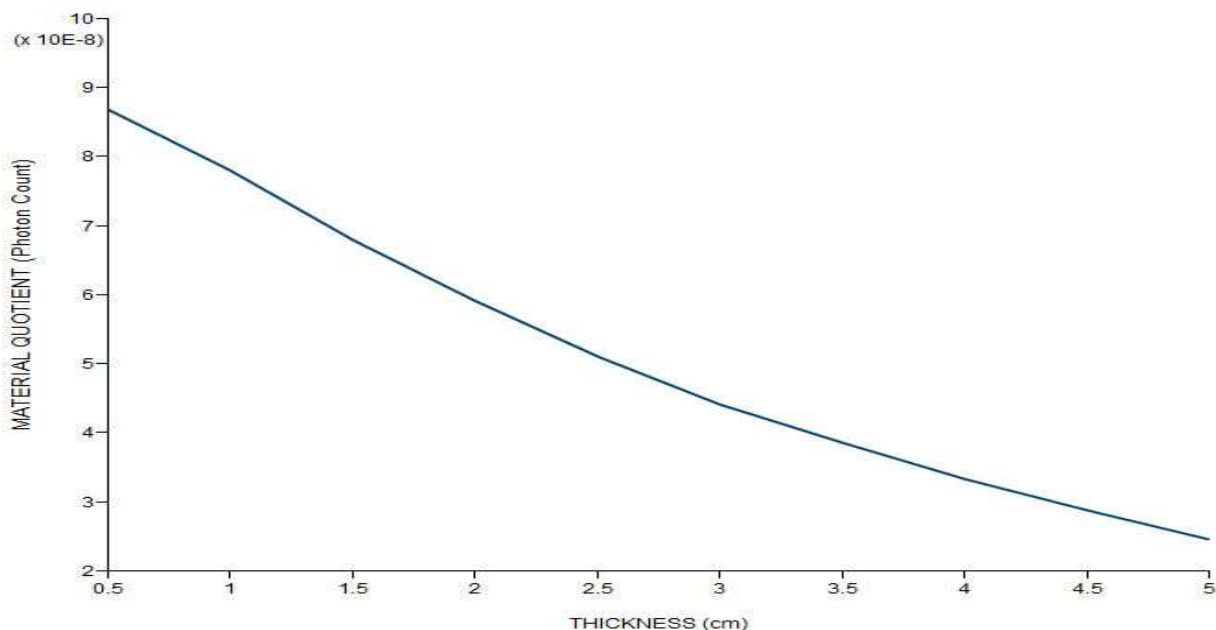


Figure 4: MQ variation with thickness for steel containers

The observed values signify that wooden containers were least affected by a variation in thickness. By this it is implied that wooden containers on a general note attenuate detection the least. By way of comparison, ceramic and HDPE containers are about 2.9 times more reactive to variation in thickness than wood. Conversely, detection of encapsulated AN may be said to be about 2.9 times less dependent on the thickness of the encapsulating material in wood as it is for ceramic or HDPE. Detection in steel encapsulation on the other hand showed a relatively high dependence on container thickness. It is seen that between 0.5 cm and 5.0 cm thickness, steel encapsulation attenuates detection by about 6.93 times more than wood and about 2.40 times more than ceramic or HDPE.

Table 5: Values for the interrogation of 200 kg of AN Explosive contained in wooden containers of varying thickness

THICKNESS (cm)	0.5	1	1.5	2	2.5	3	3.5	4	4.5	5	MEAN
MQ (E-08)	9.53	9.51	9.34	9.19	9.1	8.97	8.87	8.81	8.73	8.63	9.07
%DMQ	73.03	73.08	73.56	73.99	74.25	74.63	74.9	75.08	75.29	75.59	74.34
Range	0.90										

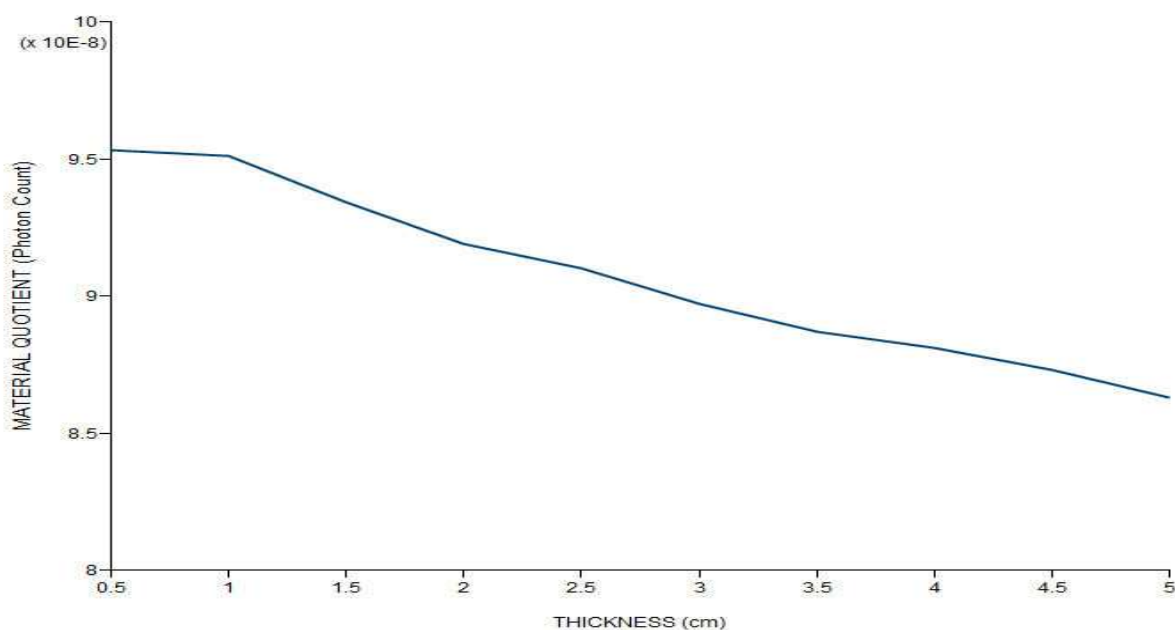


Figure 5: MQ variation with thickness for wood containers

The observed trend for wood poses a conflict between theoretical expectation and simulation result. Considering the container materials examined, wooden containers appear to present the least attenuation to detection. However, it will be observed that wood has relatively high hydrogen content and is very effective as a radiation shield. This should naturally attenuate to a great extent the particles crisscrossing its width resulting in low detection values for the explosive contained within. This is however not the trend observed. We may explain the observed trend when we acknowledge that wood has a full presence of carbon, nitrogen and oxygen (CNO) in its composition. Neutron particles passing through the target will not only activate the explosive but the container also. The photons due to the explosive charge may thus be greatly attenuated by the container. However, the surface of the container closest to the detector if activated will send in its CNO rays for detection resulting in the values observed. The high values of detection within wooden containers may thus be seen as largely due to the effect of intrinsic background contribution and not entirely that due to the explosive charge contained within the wooden encapsulation. It is noteworthy therefore that wooden materials by this reason hold a high probability of triggering false positive alarms in detection systems.

The tabulated %DMQ values are computations of the percentage deviation of individual MQ values from the MQ value for the unpacked explosive. An examination of the values indicates that %DMQ increases as container thickness increases. This implies generally that as container thickness increases, detectability decreases at an increasing rate. Ceramic has an average percentage deviation of 76.74%, HDPE 77.12%, wood 74.34%, and steel 85.50%. With the high percentage deviation from the unpacked explosive observed, it is not surprising that the issue of false alarms poses such a serious challenge to explosive detection.

5.0 Conclusion

An investigation into the effect of encapsulating materials (containers) on the detection of AN has been undertaken. Four container materials namely ceramic, HDPE, carbon steel and wood were selected as representatives of the four classes of engineering materials and their effect on detection studied. It was shown that the thickness of explosive packaging is inversely related to detectability, implying a decrease in detectability as container thickness increases. A 0.5 cm thick explosive container was found to attenuate detection by more than 70% for all materials studied. Steel encapsulated explosives were found to have the highest attenuation coefficient per unit increase in thickness. Wooden containers on the other hand pose the greatest probability of false positive alarms for detection systems.

REFERENCES

- [1] Binnie, J. and Wright, J. (2013). 'Infernal Machines': Improvised Explosive Devices. In: Small arms survey 2013, Geneva: Small arms survey, 218 - 249
- [2] Dunn, W. L., Banerjee, K., Allen, J. and Meter, V. (2007). Feasibility of a Method to identify Targets that are likely to Contain Conventional Explosives. *Nuclear Instruments and Methods in Physics Research*, Section B, 263(1), 179 –182.
- [3] GTI. (2015). *Global Terrorism Index 2015*. New York: Institute for Economics and Peace: <http://www.economicsandpeace.org>
- [4] James, E. M. (2006). *Physics for Radiation Protection: A Handbook* (2nd ed.). Weinheim: WILEY-VCH Verlag GmbH & Co., 337-341
- [5] Lamarsh, J. R. and Baratta, A. J. (2001). *Introduction to Nuclear Engineering* (3rd ed.). Upper Saddle River, New Jersey: Prentice-Hall, Inc. pp 52-61.
- [6] National Research Council. (2004). Existing Detection Techniques and Potential Applications to Standoff Detection. In: N. A. Sciences, *Existing and Potential Standoff Explosives Detection Techniques*, Washigton D.C.: National Academies Press, 71 – 96.
- [7] Sharma, S. K., Jakhar, S., Shukla, R., Shyam, A. and Rao, C. S. (2010). Explosive Detection System using Pulsed 14 MeV Neutron Source. *Fusion Engineering and Design*, 85(7), 1562–1564.
- [8] X-5 Monte Carlo Team. (2005). *MCNP – A General Monte Carlo N-Particle Transport Code, Version 5, Volume I: Overview and Theory*. Los Alamos National Laboratory, Los Alamos, New Mexico: <http://mcnp.lanl.gov/>.